International Journal of Thermophysics, Vol. 14, No. 3, 1993

Thermophysical Property Measurement at High Temperatures by Laser-Produced Plasmas[1]

Y. W. Kim[2]

Excitation by a high-power laser pulse of a material surface generates a sequence of plasma, fluid flow, and acoustic events. These are well separated in time, and their detection and analysis can lead to determination of material properties of the condensed phase target. We have developed a new methodology for real-time determination of molten metal composition by time-resolved spectroscopy of laser-produced plasmas (LPP). If the laser pulse is shaped in such a way that the movement of the bulk surface due to evaporation is kept in pace with the thermal diffusion front advancing into the interior of the target, the LPP plume becomes representative of the bulk in elemental composition. In addition, the mass loss due to LPP ablation is very well correlated with the thermal diffusivity of the target matter. For several elemental solid specimens, we show that the product of the ablation thickness and heat of formation is proportional to the thermal diffusivity per unit molecular weight. Such measurements can be extended to molten metal specimens if the mass loss by ablation, density, heat of formation, and molecular weight can be determined simultaneously. The results from the solid specimen study and the progress with a levitation-assisted molten metal experiment are presented.

KEY WORDS: laser heating; levitation; molten metal; plasma.

1. INTRODUCTION

The interaction of a high-power laser pulse with a condensed phase target results in a wide range of thermal states for the surface, vapors driven out of the surface, and the bulk. The dynamics of the matter in such laser driven states are themselves of great interest from the standpoints of nonlinear optics, nonlinear dynamics, plasma spectroscopy, atomic and molecular physics, statistical physics, and materials properties.

[1] Paper presented at the Third Workshop on Subsecond Thermophysics, September 17–18, 1992, Graz, Austria.

[2] Department of Physics, Lehigh University, Bethehem, Pennsylvania 18015, U.S.A.

0195-928X/93/0500-0397$07.00/0

Dense plasmas generated from solid targets by intense laser irradiation present a very rich array of gasdynamic and radiative phenomena [1, 2]. The spatiotemporal evolution of laser-produced plasma (LPP) is determined by the strong interplay between the gas dynamics of the species emanating from the surface, laser heating, and the radiation transport within the plasma plume. The interplay is, in general, nonlinear to the extent that each physical process may be modified by the others. Such a strong interplay leads to a complex spatiotemporal evolution of the plasma. As a consequence, we have observed, for example, a strong anisotropy in the radiation transport within a laser produced plasma. The characteristics of the optical radiation from the plasma plume have been detailed on the basis of emission spectroscopy, resolved in time, space, and direction [3].

The laser-produced vapor plume has also been recognized as the source of the future for fabrication of semiconductor devices, high-T_c superconductors, and other forbidden states of matter. Under certain conditions it becomes possible to generate an LPP which is representative of the bulk in a condensed phase. The plasma then provides an opportunity for rapid *in situ* determination of the elemental composition of the bulk and opens the way to compositional control sensors for materials in a process stream. Another possibility is to exploit the nature of laser–matter interaction in order to modify the elemental composition of a bulk specimen over a thickness comparable to the depth of the laser–matter interaction zone.

The physics of laser–matter interaction has many active research issues of fundamental significance. It is also of great practical interest in view of the numerous applications possible of the laser produced plasmas as mentioned above. In this paper we first treat the critical mechanisms involved in the production of the LPP plume and develop a rule of thumb for controlling the elemental composition of the plume for a given bulk target. Two examples of applications are discussed: elemental composition analysis of metallic alloys and measurement of thermophysical properties of metals at high temperatures.

2. PHYSICS OF LASER–MATTER INTERACTION

When elemental metallic targets are exposed to laser excitation at power densities in the range of 10^9 to $10^{11}\,\mathrm{W\cdot cm^{-2}}$, extremely dense and energetic plasma plumes, exceeding $10^{21}\,\mathrm{cm^{-3}}$ in electron density at the peak and several hundred electron volts in core temperature, are produced. Such properties can be determined from the second harmonic generation, measurement of ion acoustic wave frequency, plasma spectroscopy, and numerical simulation. Streak photography, utilizing an intensified streak tube camera, shows two distinct stages of the plasma plume development: a

"fast ion" plasma, with a radial expansion velocity reaching $2.5 \times 10^7 \text{ cm} \cdot \text{s}^{-1}$, and a plasma core, which evolves more slowly [4]. A strong shock wave develops due to the expansion of the plasma core into the remnant gaseous atmosphere of the fast ion plasma. The shock speed may be as high as $5 \times 10^6 \text{ cm} \cdot \text{s}^{-1}$.

The so-called fast ion plasma is of a curious origin. The mechanism is generally thought to involve a multiphoton process at the condensed-phase surface or within the bulk close to the surface. There is some evidence that this process takes place distinctly separately from the thermal heating process of the plasma plume production [5]. At laser power densities of 10^5 or $10^6 \text{ W} \cdot \text{cm}^{-2}$, well below the laser breakdown threshold, singly ionized ions of the bulk elements are detected with kinetic energies equivalent to the energy of N photons less a core electron binding energy. Here N is an integer in the range of 10 to 20, depending on the excimer laser wavelength and the binding energy. Given such a connection to ionization by core electronic excitation, similar to the Auger process, one would expect a strong elemental dependence of N for a given wavelength and of the threshold power density. This is indeed the case according to the time-of-flight mass and energy analysis. The elemental dependence has an interesting consequence in that the rate at which ions can be extracted from the bulk target will differ according to elemental species.

It is, however, not clear as to how the multiphoton process proceeds at higher laser power densities, where heating of the surface and the resultant vapor plume, through absorption of the laser power in the linear regime, becomes dominant. It is possible that a multiphoton process, at a smaller N value, comes into play within the vapor plume as well, providing the seed electrons necessary for direct heating of the plume by the inverse Bremsstrahlung process to take effect. There is some support for this possibility: another earlier mass spectrometric study of the LPP plume showed an increasingly peaked angular distribution of ions with increasing stages of ionization, directed toward the laser, with the growth of the plume (see the references cited in Ref. 2). We expect that the multiphoton and thermal heating process will compete according to the elemental composition of the target surface and the laser power density.

In the power density regime of interest where robust LPP plume is produced, both the fast ion plasma and the thermal plasma are initiated essentially simultaneously. When the target is placed in an ambient gas, the thermal plasma core drives a strong shock wave. The structure of the shock front becomes complex later when the plasma core becomes supercritical and the epicenter of laser heating moves off the target surface [4]. The shock exists even when the target is placed in a vacuum because of the gaseous medium created by the fast ion plasma.

Ablation of the bulk matter during an LPP event is due primarily to the growth of the thermal plasma core. Production of the thermal plasma plume from a metallic alloy target in vacuum begins with heating of the metal surface by absorption of the laser energy in the leading edge of the laser pulse. Evaporation of the surface layer follows, according to the element-specific rate of evaporation. The surface temperature is kept in check during this stage by thermal conduction into the bulk of the condensed and gaseous phase medium, expenditure of the heat of vaporization, and radiative cooling. Transport of the evaporated species defines the growing density profile which develops into the open space away from the surface, generally with element-dependent transport coefficients. As the heating rate is increased steeply according to the laser pulse shape, the surface temperature is raised rapidly to a point where the layer of the gas-phase species at the interface begins to be thermally ionized. In fact, at large laser power densities the surface temperature can exceed the critical temperature of the bulk material because neither the evaporation nor thermal diffusion can keep up with the rate of heating.

The onset of ionization, i.e., the birth of a weakly ionized plasma, initiates direct heating of the plume by the inverse Bremsstrahlung process. The remainder of the laser pulse energy is then directed increasingly to the plasma and less to the surface. For sufficiently large laser powers, the plasma can attain the critical electron density state above which the plasma frequency exceeds the laser frequency, thus preventing the laser from heating the surface.

From the standpoint of materials analysis and processing, there is a balance to be achieved between the laser energy used for ablation of the bulk material into the plasma and that for direct heating of the plasma. When it is out of an optimum balance, the elemental density in the plasma may be high enough but the plasma temperature is too low, or the temperature is high enough but the density is not. Since the intensity of an emission line is proportional to the population in the upper excited state of the radiating species, as determined by both the number density of the species in the plasma and the temperature, any imbalance directly affects the sensitivity, signal-to-noise ratio, and reproducibility of concentration determination by quantitative spectroscopy of the LPP plume. The kinetic energy of the LPP plume species affects their subsequent coalescence into molecular clusters and the nature of the thin film deposition on a sustrate surface.

3. CRITERION FOR REPRESENTATIVE PLUME PRODUCTION

Production of an LPP plume whose composition is the same as that of a multielement target is necessary for both materials analysis and processing

applications. The necessary and sufficient condition for a representative LPP plume can be defined in terms of the laser pulse power profile. In this regard, it is important to recognize that the bulk surface moves as the evaporation proceeds. If the velocity of the interface movement is small compared with the thermal diffusion velocity, the evaporation takes place preferentially for those species of high evaporation rates. The result would be an LPP plume of elemental composition which is different from that of the bulk. As the surface heating rate is raised and the movement of the bulk surface speeded up, the dependence of the evaporation rate on elemental species disappears. If the laser heating rate is increased beyond this point significantly, the laser beam becomes disconnected from the surface due to its direct coupling to the plasma as discussed earlier. The plasma emission spectrum becomes dominated by the continuum emission due to the plasma processes, in contrast to the atomic contributions.

The criterion is then to choose the laser pulse power profile in such a way that the movement due to evaporation of the bulk surface is kept in pace with the thermal diffusion front advancing into the interior of the target. When this rule of thumb, as we call it, is in effect, the LPP plume becomes representative of the bulk in elemental composition. It also becomes spectroscopically productive and robust. The process of LPP production is driven by the heating characteristics of the laser pulse subject to the rule of thumb.

The physics of LPP production discussed above have been established through a critical comparison of theoretical predictions by numerical simulation [6] with detailed laboratory measurements [7]. The basic experimental arrangement and kinds of diagnostics involved are shown schematically in Fig. 1. The specific measurable events of interest are the formation of a shock wave, expansion of the luminosity front, attainment of the critical electron density, size of the LPP plume, and onset of its collapse. We have carried out such a comparison successfully for a nearly pure iron target in argon at 100-μm Hg pressure. The highlights are given in the following.

(i) The code predicts the shock wave to reach the planar region 3 mm away from the target surface at 20 ns after the initiation of the laser pulse; the measurement shows 18 ns [4].

(ii) The code predicts the expansion velocity of the luminosity front to reach 6.1×10^6 cm $\cdot$ s^{-1} at 3 mm away from the surface between 100 and 300 ns, whereas streak photography shows that the constant luminosity front expands at 6.4×10^6 cm $\cdot$ s^{-1} over the same time period.

(iii) The code indicates the electron density to rise to its critical value for the laser wavelength of 1.06 μm at 30 ns; the onset of the

second harmonic generation at 0.53 μm of the incident laser, the prerequisite being the critical plasma density, has been observed to be at 35 ns after the laser pulse initiation.

(iv) The code predicts the size of the plume, as defined by the luminosity edge, to reach 2.5 cm in radius, whereas the measured size by streak photography is about 2.2 cm.

(v) The code predicts the collapse of the luminosity edge to begin at about 400 ns, in agreement with the experiment.

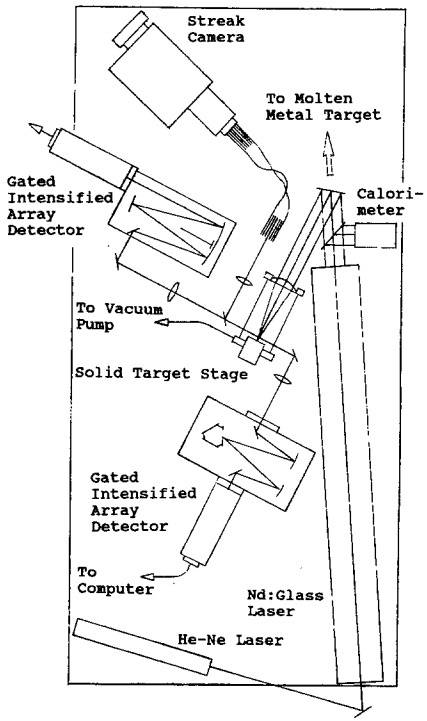

Fig. 1. A schematic diagram of the experimental setup. The primary components are shown as arranged on an optical table of 120×240-cm area. Not shown is a large array of support and diagnostic instruments such as high-speed multichannel digitizers, digital signal processors, time delay generators, high-voltage pulse generators, molten metal source, additional spectrographs, miscellaneous detectors, and vaccum stations.

An important conclusion which can be constructed from the numerical code so verified is the rule of thumb. The rule highlights the importance of the rate of mass removal from the surface.

4. THERMOPHYSICAL PROPERTY MEASUREMENT ON SOLID MATERIALS

Given that the conditions of the rule of thumb are met, it is quite clear that the rate of mass removal goes as the thermal diffusivity of the target matter, subject to the energy cost of evaporation and the plasma plume's ability to disperse away from the target surface so that the evaporation process can continue. This means that the thickness of surface ablation scales inversely with the heat of formation. It also scales with the molecular speeds in the plasma plume, i.e., decreases with increasing molecular weight. The measured thicknesses of ablation for four targets, aluminum, copper, manganese, and lead, together with the elemental properties are tabulated in Table I. In Fig. 2, we show a log–log plot of the product of the thickness and the heat of formation against the thermal diffusivity per unit molecular mass of the target for the four elements. It clearly demonstrates the scaling relation for the rate of mass removal at a constant laser pulse energy, reaffirming the physics involved in an all-inclusive manner.

Table I. Surface Matter Removal by LPP Excitation at a Constant Laser Energy of 3.5 J per Pulse

Specimen	Al	Cu	Mg	Pn
Mass removed (50 shots), mg	1	4	3	2
Thickness per shot, μm	$2.8 \pm 40\%$	$3.3 \pm 10\%$	$13 \pm 15\%$	$1.3 \pm 20\%$
Atomic weight	27	64	24	207
Atomic number	13	29	12	82
Mass density, $g \cdot cm^{-3}$	2.7	8.95	1.73	11.5
Reflectance at 1 μm, %	94	90	74	80
Thermal conductivity, $W \cdot cm^{-1} \cdot K^{-1}$	94	168	146	17
Thermal diffusivity, $cm^2 \cdot s^{-1}$	0.32	0.43	0.66	0.11
Heat of formation, $10^4 J \cdot g^{-1}$	1.34	0.49	0.56	0.088

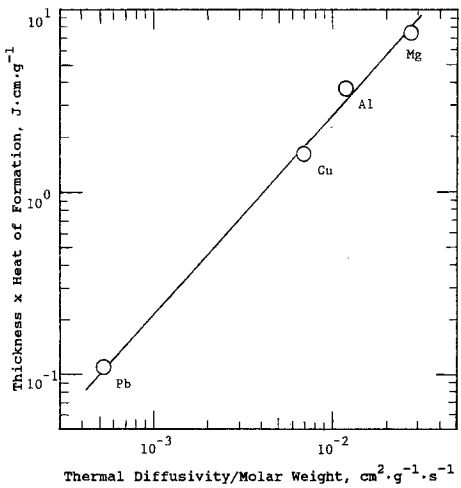

Fig. 2. A log–log plot of the product of ablation thickness per laser shot and the heat of formation against the thermal diffusivity per unit molar weight of the target material.

It is now possible to extend this as a general method of thermal diffusivity measurement for arbitrary materials. The material does not have to be pure elemental substance. It may be an alloy of many elemental species, in which case its elemental composition can be determined by time- and space-resolved spectroscopy of the LPP plume, while the ablation loss is determined simultaneously. The analysis is not restricted to metallic substances either, as long as the transparency does not enter into the energy transport in a dominant way. For transparent materials the window of application can be defined in a different part of the parameter space. We do not, however, address such cases here.

5. THERMOPHYSICAL PROPERTY MEASUREMENT ON MOLTEN MATERIALS

We have begun to extend the above LPP method for themophysical property measurement to those materials in a molten state. As the first requirement of producing the molten state which is reproducible and characterizable, we have developed a levitation-assisted molten metal source. It is powered by an RF power generator, rated for 7.5 kW and operating at frequencies from 70 to 200 kHz. The basic coil has three turns and a fourth turn in reverse at the top so as to create a minimum B-field zone. The diameter of the levitator coil is about 3.0 cm at its maximum.

A metallic specimen of 6.4-mm diameter and 5.0-cm length is placed vertically just below the minimum-B point. The top end is heated to melting while supported by the leviation field; this prevents the molten metal from spilling over. The overall construction of the levitation-assisted molten metal source is shown schematically in Fig. 3.

Laser excitation takes place at the top surface of the molten specimen. The time- and space-resolved spectroscopic diagnostics can be performed of the LPP plume from the molten surface. Overall, the characteristics are similar to those for the solid specimen except that (i) the reflectance is higher in the molten state than in the solid state for the same material specimen, and (ii) the heat of formation for melting is not involved in the formation of the LPP plume from the molten target, unlike that with a

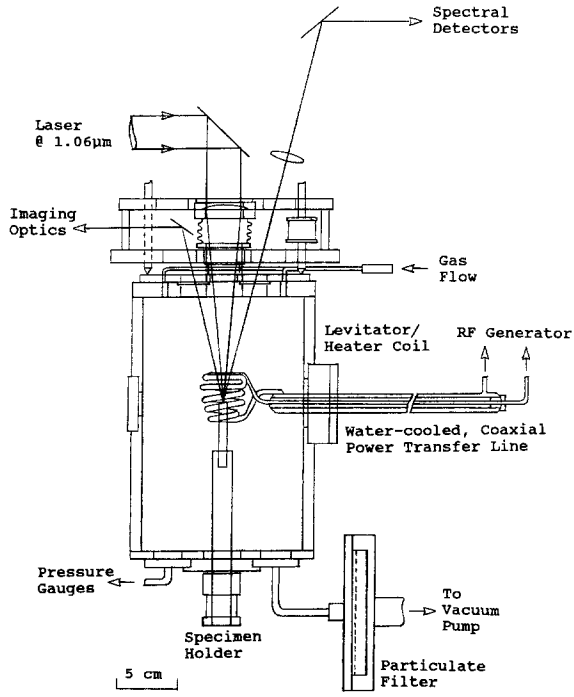

Fig. 3. A schematic diagram of the levitation-assisted molten metal source. Normally, a metallic specimen, 6.4 mm in diameter and 5.0 cm in length, is mounted on the specimen holder. The top end of the specimen is brought to melting by RF heating within 20 to 30 s, depending on the material properties of the specimen. After each laser excitation, the molten end is resolidified and the specimen is recovered for further analysis. The fully molten state lasts no longer than 5 s.

solid target. We have confirmed that all of the signatures are consistent with the rule of thumb for LPP plume production.

The quantitative spectroscopy of the LPP plume provides the elemental composition and thus the molecular weight. The heat of formation can be deduced in reference to the solid state. Finally, the ablated mass or thickness per laser excitation may be determined from the impulse imparted on the target and the mean velocity of the LPP plume or the temperature deduced from plasma spectroscopy. The impulse measurement can take a number of different forms. We are currently implementing an approach based on a high speed piezoelectric transducer mounted on the specimen holder just below the target specimen. In practice, we anticipate that the impulse measurement can be calibrated to provide the ablative mass loss through the use of a set of solid specimen standards.

6. CONCLUSION

Establishment of the criterion for representative LPP plume, or the rule of thumb, makes it possible to strategize applications of laser-produced plasmas in a number of areas. In view of the high plasma temperature and density achievable, the LPP plume is spectroscopically robust and, as a result, well suited for elemental composition analysis of condensed-phase alloys and composites. We have successfully developed a new methodology, as well as the hardware for a sensor-probe, for real-time, *in situ* analysis of molten metal alloys [8, 9].

On the other side of the issue lies the possibility of exploring the composition inhomogeneity by the LPP sensor probe. The examples of interest are a depth dependence of elemental composition in thin film alloys and elemental segregation due to heterogeneous nucleation in alloys [7]. In view of the precision with which a layer of surface matter can be removed by a laser pulse under the rule of thumb, the elemental composition can be determined one layer after another by successive LPP excitation. This analysis can take place as a function of depth or across the surface. We have implemented this for surface composition profiling and mapping of segregation in steel alloys with distance resolution of a tenth of a micron. The overall sensitivity is in excess of 1 part in 10 million in concentration and the reproducibility is $\pm 2\%$ for solids and $\pm 4\%$ for molten metal alloys. We expect that these performance figures can be further improved by a factor of 5 or 10, well exceeding the performance figures of the conventional analysis approaches. Such studies will be able to provide the microscopic basis for theoretically treating thermophysical properties such as surface tension, emissivity, heat transfer coefficient, shear viscosity, etc.

Another major area of application is to utilize the LPP plume as a source of multielement vapors for thin film deposition. Of particular interest is the fabrication of high-T_c superconducting thin films using a target of stoichiometric metal oxide blends and an excimer laser as a laser pulse power source [10]. It is also possible to exploit the threshold behavior of the multiphoton ion production mechanism for element-selective trimming of the thin film; the composition profile can also be modified in this manner [11]. Again, thermophysical properties of thin films can be explored by the method presented here.

There are more applications envisioned for other metallic, ceramic, and polymeric materials processing, surface reaction studies [12], atomization, plasma deposition, and etching. The relevant questions are how such transient processes influence thermophysical properties, and the LPP method will be a useful approach for addressing them.

ACKNOWLEDGMENTS

The author acknowledges the valuable contributions of his students and colleagues: K.-S. Lyu, C. S. Park, S. H. Kim, C. Lloyd-Knight, J. Gregoris, and D. Xie. This work was supported in part by the American Iron and Steel Institute, U.S. Department of Energy, Ben Franklin Fund, Electric Power Research Institute through Center for Materials Production, and Lehigh University.

REFERENCES

1. J. L. Bobin, *Phys. Rep.* **122**:173 (1985).
2. Y. W. Kim, in *Laser-Induced Plasmas and Applications*, L. J. Radziemski and D. A. Cremers, eds. (Marcell Dekker, New York, 1989), Chap. 8.
2. Y. W. Kim, in *Proceedings of the 18th International Symposium on Shock Waves, Sendai, Japan, July 20–26, 1991* (in press).
4. Y. W. Kim, K.-S. Lyu, and J. C. Kralik, in *Current Topics in Shock Waves*, AIP Conference Proceedings 208, Y. W. Kim, ed. (American Institute of Physics, New York, 1990), pp. 353–358.
5. H. Helvajian and R. Welle, *J. Chem. Phys.* **91**:2616 (1989).
6. K.-S. Lyu, *Non-Linear Processes in Laser-Produced Dense Plasma*, Ph.D. dissertation (Lehigh University, Bethlehem, PA, 1988).
7. Y. W. Kim, in *Advanced Sensing, Modelling and Control of Materials Processing*, E. F. Mathys and B. Kushner, eds. (Minerals, Metals and Materials Society, Warrendale, PA, 1992), pp. 45–57.
8. Y. W. Kim, in *Intelligent Processing of Materials*, H. G. N. Wadley and W. E. Eckhart, eds. Minerals, Metals and Materials Society, Warrendale, PA, 1990), pp. 317–327.

9. Y. W. Kim, *High Temp. Sci.* **26**:57 (1990).
10. A. Inam, M. S. Hegde, X. D. Wu, T. Venkadesan, P. England, P. F. Miceli, E. W. Chase, C. C. Chang, J. M. Tarascon, and J. B. Wachtman, *Appl. Phys. Lett.* **53**:908 (1988).
11. L. Wiedeman and H. Helvajian, *Mat. Res. Soc. Symp. Proc.* **191**:217 (1990).
12. Y. W. Kim, in *Proceedings of the Symposium on High Temperature Materials Chemistry-V*, W. B. Johnson and R. A. Rapp, eds. (Electrochemical Society, Pennington, NJ, 1990), pp. 175–184.